

Self-assembled InAs quantum wire lasers on (001)InP at 1.6 μm

F. Suárez,^{a)} D. Fuster, L. González, Y. González, J. M. García, and M. L. Dotor
Instituto de Microelectrónica de Madrid (CSIC), Isaac Newton 8, PTM 28760 Tres Cantos, Madrid

(Received 17 May 2006; accepted 3 July 2006; published online 1 September 2006)

In this work, the authors present results on the growth by atomic layer molecular beam epitaxy and characterization of lasers with one and three stacked layers of InAs quantum wires (QWRs) as active zone and aluminum-free waveguides on (001) InP substrates. The separated confinement heterostructure consists of *n-p* InP claddings and a waveguide formed by short period superlattices of $(\text{InP})_5/(\text{GaInAs})_4$ lattice matched to the InP substrate. The optimum growth conditions (substrate temperature and As and P pressures) have been determined to obtain waveguides with a flat surface in order to get a uniform QWR distribution. Lasing emission is observed at a wavelength of $\sim 1.66 \mu\text{m}$ up to 270 K from $15 \times 3000 \mu\text{m}^2$ devices, with a threshold current density at that temperature of 2 kA/cm². © 2006 American Institute of Physics. [DOI: 10.1063/1.2335775]

In recent years there has been a large and growing interest in employing semiconductor self-assembled nanostructures in optoelectronics devices such as lasers, photodetectors, and amplifiers, and in exploiting their unique electrical and optical properties compared with conventional quantum well structures. As an example, during the last years, many of the characteristics of quantum dot (QD) lasers have been improved: low threshold current densities, reduced temperature sensitivity, ultrawide gain bandwidth, and reduced chirp.^{1–3} With the most studied material system (InAs QD on GaAs), it is possible to reach wavelengths longer than 1 μm . However, with this system it is nontrivial to go beyond 1.3 μm due to the large (7%) lattice mismatch between InAs and GaAs, which is a very serious problem that has to be overcome for a realistic use of these materials in devices. Some recent results have shown optical emission at 1.6 μm at room temperature (RT) using QD of InAs on GaAs capped with GaInAs and GaAsSb.^{4–6} Unfortunately these nanostructures have two main problems: low efficient photoluminescence and type II band gap alignment when Sb based materials are employed.

As an alternative, InAs nanostructures on InP (100)-oriented substrates (with a lattice mismatch of 3%) are a promising technology for developing very efficient devices that could easily reach longer wavelengths ($>1.55 \mu\text{m}$) and which could be rapidly transferred into practical applications such as optical telecommunications (1.55 μm), gas sensing, and molecular spectroscopy (1.8–1.9 μm).^{7,8}

When a small amount [~ 2 –10 ML (monolayer)] of InAs is deposited on InP, the type of nanostructures that can be obtained strongly depends on substrate orientation and growing techniques. For example, high density dots are formed on InP(001) by low-pressure metal-organic vapor-phase epitaxy⁹ and metal-organic chemical vapor deposition.¹⁰ When solid source molecular beam epitaxy (MBE) is employed, the growth details determine the type of nanostructures that are formed. For example, one can obtain either a dashlike or a dotlike shape on InAlAs buffer layers lattice matched to InP,^{11,12} while on (001) InP buffer layers, the formation of quantum wires (QWRs) has been continuously reported.^{13,14} It has been proposed that the wires are elongated along the [1–10] direction as an effective way to

relax the intrinsic strain asymmetry in $\langle 110 \rangle$ directions built-in at the InAs/InP interface under V-element stabilized growth conditions.¹⁵ A similar mechanism would explain the QWR formation in the case of GaAs growth by chemical beam epitaxy on (001)GaP.¹⁶

One important and unavoidable characteristic of InAs/InP system is related to processes of exchange between As and P. These processes are present both during InAs nanostructure formation and during the capping of the QWR, controlling the final vertical size of the capped wires. Consequently, As/P exchange processes can be used to tune the QWR optical emission.¹⁷ Changing the substrate temperature is a reliable way to control this exchange process. So growing the InP cap layer at high temperatures ($\geq 500 \text{ }^\circ\text{C}$) results in a large P/As exchange to take place, reducing the effective vertical size in such a way that a lower emission wavelength is achieved. On the other hand, a low growth temperature of the InP cap layer ($\leq 450 \text{ }^\circ\text{C}$) causes a negligible exchange to take place, leading to higher nanostructures and therefore to longer wavelength emission.

At present, quantum-dash lasers with AlGaInAs waveguides and AlInAs claddings on (001)InP showing RT emission at $\sim 1.6 \mu\text{m}$ with a threshold current density (J_{th}) of 410–500 A/cm² have been demonstrated.^{8,18} However, quaternary and ternary alloys containing aluminum in the laser structures have bad aging properties and should be avoided in ideal laser devices. Paranthoen *et al.* have obtained state of the art 1.52 μm laser devices using high density dots formed by gas source MBE on (311)B InP substrates.¹⁹ As a drawback, the use of misoriented substrates presents a technological barrier for its industrial implementation as mirror cleaving and etching processes are not standard.

In this work we present results on the growth by atomic layer MBE (ALMBE) of aluminum-free laser structures with InAs QWR as active zone on (001) InP substrates, device processing, and the characterization of lasers.

The laser epitaxy has a separated confinement heterostructure that consists of a waveguide formed by $(\text{InP})_5/(\text{GaInAs})_4$ short period superlattice (SPSL) lattice matched to (001) InP substrate. As previously demonstrated, the growth by means of ALMBE of SPSL and cladding layers has several advantages such as sharp interfaces, reduced segregation of dopants, enhancement of the electrical characteristics, and improvement of T_0 values by a factor of

^{a)}Electronic mail: ferran@imm.cnm.csic.es

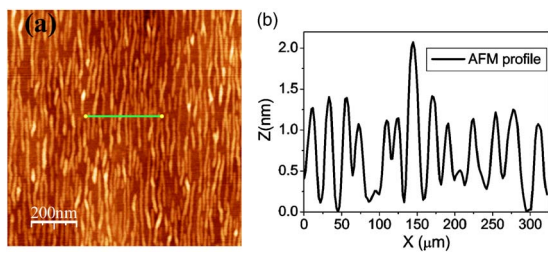


FIG. 1. (a) $1 \mu\text{m}^2$ size atomic force microscopy (AFM) image and (b) AFM profile of uncapped quantum wire (QWR) grown on top of a short period superlattice. QWR are oriented along the $[1-10]$ direction and have 1.2 nm height and 18 nm pitch period.

1.3.^{20,21} Contact mode atomic force microscopy (AFM) characterization has been used to study the surface morphology of superlattice samples grown under various values of As_4 and P_2 beam equivalent pressures (BEPs) at a fixed substrate temperature (405°C), looking for a flat SPSL surface that is crucial for the formation of homogeneous QWR.²² The optimum growth conditions for high quality InP/GaInAs SPSL are BEPs of $P_2=3.6 \times 10^{-6}$ mbar and $As_4=2.35 \times 10^{-6}$ mbar and substrate temperature $T_s=405^\circ\text{C}$. Under these growth conditions we obtain SPSL with a root mean square roughness of only 0.4 nm in a $5 \times 5 \mu\text{m}^2$ area. Figure 1(a) shows an AFM image of a sample with a layer of QWR grown on top of the optimized SPSL. The average vertical size of the wires is 1.2 nm and the average pitch period is 18 nm [Fig. 1(b)]. These results demonstrate that QWR similar to those obtained on InP (Refs. 7, 17, and 22) can be grown on top of SPSL waveguides.

The laser structures are grown on S-doped (001) InP substrates. The waveguide is a 320 nm thick SPSL $(\text{InP})_5/(\text{Ga}_{0.45}\text{In}_{0.53}\text{As})_4$ and the active region consists of either a single or three stacked layers of QWR, respectively. The InP cladding layers (1 μm thick) are Si ($n=1 \times 10^{18} \text{ cm}^{-3}$) and Be doped ($p=1 \times 10^{18} \text{ cm}^{-3}$). A 50 nm thick $\text{Ga}_{0.47}\text{In}_{0.53}\text{As}:\text{Be}$ ($p=1 \times 10^{19} \text{ cm}^{-3}$) layer was grown on top in order to provide good quality electrical contacts to the p -type layers. InP claddings were grown by ALMBE at 350°C . For the waveguide the above described optimized growth conditions were used. The QWR, situated at the center of the waveguide, was grown on top of an InP terminated period of the SPSL. To form the QWR, 2.3 ML of InAs at 405°C were deposited followed by an annealing at 515°C under As_4 flux until a two-dimensional to three-dimensional transition, associated with the QWR assembly, is observed in the reflection high-energy electron diffraction pattern.²² For the samples containing three stacked layers of QWR, the SPSL spacer layer thickness is 20 nm. Broad area lasers (40 μm stripe width) and 15 μm ridge lasers were fabricated to measure the threshold current and lasing spectrum. Au-Ge-Au and Ti/Pt/Au metals were used for the n and p contacts, respectively. The cavity length (L) ranging from 1 to 3 mm long are formed by edge cleaving along $[1-10]$ direction. The lasing threshold was obtained by measuring the light-current characteristic with a GaInAs detector under pulsed operation (pulse width of 1–5 μs and duty cycle of 0.1%–0.08%, respectively) with the devices in a close cycle helium cryostat. The collected signal was spectrally dispersed with a double 0.75 m focal length monochromator.

Figure 2 shows the light output characteristic at 200 K of a 3 mm long broad area laser, with three stacked layers of QWR in the active region. The threshold current density is

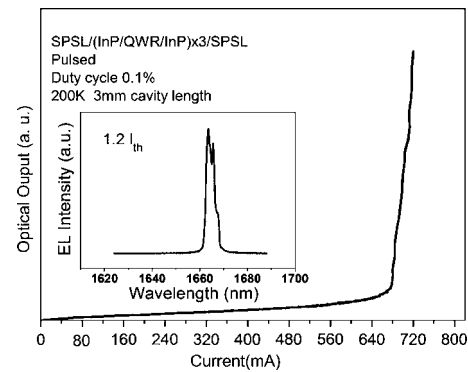


FIG. 2. Laser characteristics (optical output vs injection current). The inset shows the lasing spectrum from a 3 mm long and 40 μm wide laser diode, with three stacked layers of quantum wires in the active region.

558 A/cm^2 , which is equivalent to 186 A/cm^2 per QWR layer. The electroluminescence spectrum is shown in the inset of Fig. 2 at 200 K with an injection current of 1.2 times the threshold current ($I=1100 \text{ mA}$) the threshold current (I_{th}). The laser emission is centered at a wavelength of $1.665 \mu\text{m}$ with a multimodal distribution typical of broad area laser.

Figure 3 shows the electroluminescence (EL) spectra of a broad area laser with three stacked layers of QWR in pulse operation at 200 K for injection currents from 35 to 1040 mA ($1.08I_{th}$). The EL emission consists of a broad peak that shifts from 1750 nm (0.700 eV) to 1620 nm (0.765 eV) as the injection current is increased. This behavior can be due to the presence of several families of QWR with 1 ML difference in height.^{23,24} At low injection currents, only the recombination of the ground energy levels is observed. As the injection current increases the ground energy levels begin to saturate and excited energy levels start to contribute to the EL signal. Stimulated emission is observed above 820 mA at 1610 nm, probably associated with emission from excited states. The gain of ground states is saturated but that of the excited states is not, and consistently, lasing is present at lower wavelengths when the gain exceeds the losses in the threshold.

Figure 4 shows the measured values of J_{th} versus temperature of broad area devices from two laser epitaxies with a single layer and three stacked layers of QWR as active region, processed with $L=1, 2,$ and 3 mm. As can be observed, laser devices with three stacked layers of QWR have a lower threshold current than lasers with a single layer of QWR. Similar results are reported in InAs/GaAs QD lasers

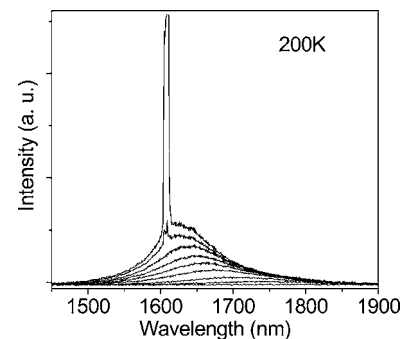


FIG. 3. Electroluminescence spectra of three stacked layers of QWR laser, with cavity length $L=2 \text{ mm}$ for injection currents of 35, 90, 200, 390, 540, 640, 820, 960, and 1040 mA at 200 K. Above 820 mA lasing emission is observed at 1610 nm.

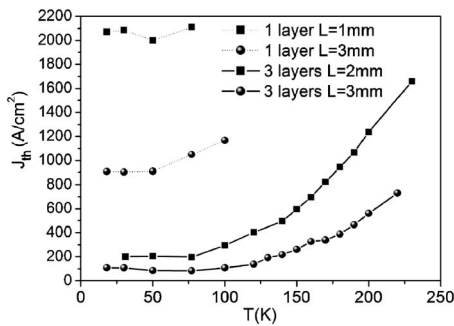


FIG. 4. Threshold current density (J_{th}) vs T of two laser devices containing a single layer and three stacked layers of quantum wires in the active region. Laser devices with cavity lengths of 1, 2, and 3 mm are shown.

and InAs/InP Q-dash laser,⁶ and are commonly associated with an increase in the modal gain due to an increase in the optical confinement factor (Γ). Also, laser with longer L have lower threshold current density because the optical losses decrease with L .

Our results for the laser structure with a single layer of QWR show a rapid saturation in the optical gain that inhibits laser emission at the energy levels of QWR for devices with $L \leq 1$ mm. Stimulated emission from a single layer of QWR device with $L=1$ mm, measured at 1172 nm (in the range of 18–100 K), corresponds to the waveguide. Same laser structure with $L=3$ mm has a J_{th} 2.3 times lower and shows stimulated emission around 1430 nm (in the range of 18–100 K) from QWR excited energy levels.

Lasers with three stacked layers of QWR show emission at 1645–1665 nm (in the range of 18–200 K) from QWR energy levels for devices with $L=3$ and 2 mm, respectively. These devices show threshold density currents that are one order of magnitude lower than lasers with single layer of QWR. The maximum operating temperature for these lasers is 220–270 K, while that with a single layer of QWR is ~ 100 K. Nevertheless, in order to get lasing emission at RT higher injection currents are needed, in which case thermal heating effects become more important. Stimulated emission is still observed at 270 K from $15 \times 3000 \mu\text{m}^2$ devices, when the duty cycle is reduced down to 0.08% with a threshold current of 2 kA/cm².

With respect to the characteristic temperature (T_0) values measured from 77 to 230 K in these three stacked layers of QWR broad area devices, we obtained 71 and 74 K for $L=2$ and 3 mm, respectively. These values of the T_0 are not so high as expected because the laser emission came from excited states of the QWR, and the thermal escape of the carriers from these levels to the barriers increases the threshold current when the temperature is increased.

In our opinion several improvements should be considered in the design of the QWR based laser epitaxial structures in order to obtain better devices: (a) stacking more than three layers of QWR in order to increase the modal gain; (b) growing asymmetric energy barriers above and below the nanostructures to selectively block the escape of carriers from the nanostructures,²⁵ which could help in reducing the thermal escape of carriers without limiting their injection; and (c) introducing a p delta doping close to the nanostructures in order to have a very high efficient injection of holes and avoid transport losses.²⁶

In summary, uniform QWR growth on SPSL waveguides has been demonstrated and has been used to fabricate QWR

lasers on (001) InP substrates with Al-free waveguides of (InP)₅/(GaInAs)₄ with laser emission at $\sim 1.66 \mu\text{m}$ at 270 K. The threshold current of the devices is reduced by one order of magnitude with respect to a single layer of QWR by stacking three layers of QWR.

More studies of quantum wire growth on superlattices are necessary to reduce the broadening of the EL emission in order to assure lasing from ground states and therefore low threshold currents.

This work was financed by Spanish project Nos. MEC TEC-2005-05781-C03-01 and CAM S_0505ESP_0200, by the SANDIE Network of excellence (Contract No. NMP4-CT-2004-500101), and by the European Commission Growth program NANOMAT project, Contract No. G5RD-CT-2001-00545.

¹M. Henini and M. Bugajskib, *Microelectron. J.* **36**, 950 (2005).

²J. H. Marsh, D. Bhattacharyya, A. Saher Helmy, E. A. Avrutin, and A. C. Bryce, *Physica E (Amsterdam)* **8**, 163 (2000).

³V. M. Ustinov, A. Yu. Egorov, A. R. Kovsh, A. E. Zhukov, M. V. Maximov, A. F. Tsatsulnikov, N. Yu. Gordeev, S. V. Zaitseva, Yu. M. Shernyakov, N. A. Bert, P. S. Kop'ev, Zh. I. Alferov, N. N. Ledentsov I, J. Brhrer, D. Bimberg, A. O. Kosogov, P. Werner, and U. Grsele, *J. Cryst. Growth* **175/176**, 689 (1997).

⁴E. C. Le Ru, P. Howe, T. S. Jones, and R. Murray, *Phys. Status Solidi C* **0**, 1221 (2003).

⁵J. M. Ripalda, D. Granados, Y. González, A. M. Sánchez, S. I. Molina, and J. M. García, *Appl. Phys. Lett.* **87**, 202108 (2005).

⁶H. Y. Llua, M. J. Steer, J. Badcock, D. J. Mowbray, M. S. Skolnick, F. Suarez, J. S. Ng, M. Hopkinson, and J. P. R. David, *J. Appl. Phys.* **99**, 046104 (2006).

⁷David Fuster, Luisa González, Yolanda González, María Ujué González, and Juan Martínez-Pastor, *J. Appl. Phys.* **98**, 033502 (2005).

⁸R. Schwerberger, D. Gold, J. P. Reithmaier, and A. Forchel, *IEEE Photonics Technol. Lett.* **14**, 735 (2002).

⁹Yueming Qiu, David Uhl, Rebecca Chacon, and Rui Q. Yang, *Appl. Phys. Lett.* **83**, 1704 (2003).

¹⁰S. H. Pyun, S. H. Lee, I. C. Lee, H. D. Kim, Weon G. Jeong, J. W. Jang, N. J. Kim, M. S. Hwang, D. Lee, J. H. Lee, and D. K. Oh, *J. Appl. Phys.* **96**, 5766 (2004).

¹¹J. Brault, M. Gendry, G. Grenet, G. Hollinger, J. Olivares, B. Salem, T. Benyatou, and G. Bremond, *J. Appl. Phys.* **92**, 506 (2002).

¹²M. Gendry, C. Monat, J. Brault, P. Regreny, G. Holliger, B. Salem, G. Guillot, T. Benyattou, C. Bru-chevallier, G. Bremond, and O. Marty, *J. Appl. Phys.* **95**, 4761 (2004).

¹³Haeyeon Yang, P. Ballet, and G. J. Salamo, *J. Appl. Phys.* **89**, 7871 (2001).

¹⁴H. R. Gutierrez, M. A. Cotta, and M. M. G. de Carvalho, *Appl. Phys. Lett.* **79**, 3854 (2001).

¹⁵J. M. Garcia, L. Gonzalez, M. U. Gonzalez, J. P. Silveira, Y. Gonzalez, and F. Briones, *J. Cryst. Growth* **227& 228**, 975 (2001).

¹⁶B. Jonas Ohlsson and Mark S. Miller, *J. Cryst. Growth* **188**, 387 (1998).

¹⁷D. Fuster, M. U. González, Luisa González, Y. González, T. Ben, A. Ponce, S. Molina, and J. M. Pastor, *Appl. Phys. Lett.* **85**, 1424 (2004).

¹⁸R. H. Wang, A. Stintz, P. M. Varangis, T. C. Newell, H. Li, K. J. Malloy, and L. F. Lester, *IEEE Photonics Technol. Lett.* **13**, 767 (2001).

¹⁹C. Paranthoen, C. Platz, G. Moreau, N. Bertru, O. Dehaese, A. Le Corre, P. Miska, J. Even, H. Folliot, C. Labbé, G. Patriarchec, J. C. Simonb, and S. Loualichea, *J. Cryst. Growth* **251**, 230 (2003).

²⁰M. L. Dotor, P. Huertas, D. Golmayo, and F. Briones, *Appl. Phys. Lett.* **62**, 891 (1993).

²¹P. A. Postigo, D. Golmayo, H. Gómez, D. Rodríguez, and M. L. Dotor, *Jpn. J. Appl. Phys., Part 2* **41**, L010 (2002).

²²L. González, J. M. García, R. García, J. Martínez-Pastor, C. Ballesteros, and F. Briones, *Appl. Phys. Lett.* **76**, 1104 (2000).

²³B. Alén, J. Martínez-Pastor, A. García-Cristóbal, L. González, and J. M. García, *Appl. Phys. Lett.* **78**, 4025 (2001).

²⁴J. Maes, M. Hayne, Y. Sidor, B. Partoens, F. M. Peeters, Y. González, L. González, D. Fuster, J. M. García, and V. Moshchalkov, *Phys. Rev. B* **70**, 155311 (2004).

²⁵Levon V. Asryan and Serge Luryi, *Solid-State Electron.* **47**, 205 (2003).

²⁶O. B. Shchekin and D. G. Deppe, *Appl. Phys. Lett.* **80**, 5 (2002).